

Gravitational wave detection via photon-graviton scattering and quantum interference

K. Hari^{1,*} and S. Shankaranarayanan^{1,†}

¹*Department of Physics, Indian Institute of Technology Bombay, Mumbai 400076, India*

Abstract

We present a fully quantum field-theoretic framework for gravitational wave (GW) detection in which the interaction is described as photon-graviton scattering. In this picture, the GW acts as a coherent background that induces inelastic energy exchanges with the electromagnetic field — analogous to the Stokes and anti-Stokes shifts in Raman spectroscopy. We propose a detection scheme sensitive to this microscopic mechanism based on Hong-Ou-Mandel interference. We show that the scattering-induced phase shifts render frequency-entangled photon pairs distinguishable, spoiling their destructive quantum interference. GW signal is thus encoded in the modulation of photon coincidence rates rather than classical field intensity, offering a complementary quantum probe of the gravitational universe that recovers the standard classical response in the macroscopic limit.

* hari.k@iitb.ac.in

† shanki@iitb.ac.in

I. INTRODUCTION

Almost all precision measurements involving electromagnetic (EM) radiation rely on its interaction with matter — scattering processes that lead to absorption, emission, or phase shifts [1, 2]. Canonical examples, such as Compton or Thomson scattering, are rigorously understood within quantum theory [3, 4], where both the radiation and the target are treated as quantum dynamical degrees of freedom.

In stark contrast, the detection of gravitational waves (GWs) is almost exclusively analyzed within a semi-classical framework. The EM field is treated as a classical probe of a Riemannian geometry, operationally described by variations in proper distance or optical path length between test masses [5]. While this geometric optics approximation has been triumphantly validated by the LIGO-Virgo-KAGRA collaboration [6], it suffers from fundamental limitations. It is susceptible to gauge-dependent interpretations if applied naively [7], becomes inadequate in high-frequency regimes where the phonon/optical wavelength is comparable to the GW wavelength [8], and, most critically, lacks a microscopic account of how linearized gravity couples to photons.

In this work, we bridge this gap by establishing a fully field-theoretic framework for GW detection. We treat the interaction not as a classical metric perturbation stretching a baseline, but as a scattering process between quantized EM fields and gravitons. This approach addresses foundational questions regarding the coupling of gravity to quantum systems and the detectability of gravitons, a subject of longstanding theoretical interest [9–14]. Within our framework, the GW-induced signal emerges from an energy exchange — analogous to the Stokes and anti-Stokes lines in Raman scattering — where the absorption or emission of gravitons induces minute frequency shifts in the photon field [15]. We show that in the macroscopic limit, this recovers the standard interferometric phase shift, providing a quantum derivation of the classical response.

Crucially, this microscopic perspective opens new avenues for detection beyond classical intensity interferometry. We propose a detection scheme based on Hong-Ou-Mandel (HOM) interference [16], a quintessential quantum phenomenon with no classical analogue. By exploiting the extreme sensitivity of two-photon quantum interference to distinguishability, we show that the *gravitational phase* can be read out via changes in photon coincidence rates. This architecture shifts the detection paradigm from measuring the amplitude of a

classical wave to monitoring the correlations of quantum states, offering a complementary window into the gravitational universe.

II. QUANTUM DYNAMICS OF THE PHOTON-GRAVITON INTERACTION

To establish the feasibility of HOM-based detection, we derive the effective photon dynamics induced by its interaction with the graviton field. We work in the interaction picture, tracing out the graviton degrees of freedom to obtain the reduced EM density matrix. The total Hamiltonian is:

$$H = H_{\text{ph}} + H_{\text{GW}} + H_{\text{int}}. \quad (1)$$

where H_{ph} is the free EM Hamiltonian given by,

$$H_{\text{ph}} = \sum_{\mathbf{k}, \lambda} \hbar \omega_{\mathbf{k}} \hat{a}_{\mathbf{k}, \lambda}^\dagger \hat{a}_{\mathbf{k}, \lambda}, \quad (2)$$

$a_{\mathbf{k}, \lambda}$ annihilates a photon of wave vector \mathbf{k} , polarization λ , and frequency $\omega_{\mathbf{k}} = c|\mathbf{k}|$ and the vacuum energy is excluded. Similarly, the free graviton Hamiltonian is

$$H_{\text{GW}} = \sum_{\mathbf{q}, \sigma} \hbar \omega_{\mathbf{q}} \hat{b}_{\mathbf{q}, \sigma}^\dagger \hat{b}_{\mathbf{q}, \sigma}. \quad (3)$$

where $b_{\mathbf{q}, \sigma}$ annihilates a graviton of wave vector \mathbf{q} with polarization σ . In the linearized gravity regime and the Transverse-Traceless (TT) gauge, the interaction between the EM stress-energy tensor T_{EM}^{ij} and the metric perturbation h_{ij} (via minimal coupling) is given by [17, 18]:

$$H_{\text{int}} = \frac{1}{2} \int d^3x \, h_{ij}(\mathbf{x}, t) T_{\text{EM}}^{ij}(\mathbf{x}, t). \quad (4)$$

where

$$T_{\text{EM}}^{ij} = F^{i\mu} F_\mu^j - \delta^{ij} F_{\mu\nu} F^{\mu\nu} / 4. \quad (5)$$

$$h_{ij}(\mathbf{x}, t) = \sum_{\mathbf{q}, \sigma} \frac{\varepsilon_{ij}^{(\hat{\mathbf{q}}, \sigma)}}{\sqrt{(2\pi)^3 2\omega_{\mathbf{q}}}} [b_{\mathbf{q}, \sigma} e^{i(\mathbf{q} \cdot \mathbf{x} - \omega_{\mathbf{q}} t)} + \text{h.c.}] \quad (6)$$

Expanding the fields in terms of creation ($\hat{a}^\dagger, \hat{b}^\dagger$) and annihilation (a, b) operators, the interaction Hamiltonian (in the Coulomb gauge) simplifies to:

$$H_{\text{int}} \approx \frac{1}{2} \sum_{\mathbf{k}, \mathbf{q}} \sum_{\sigma, \lambda, \lambda'} \frac{\omega_{\mathbf{k}}}{(2\pi)^3 2\sqrt{\omega_{\mathbf{q}}}} g_{\mathbf{k}, \hat{\mathbf{q}}}^{\sigma, \lambda, \lambda'} \left[\hat{n}_{\mathbf{k}, \lambda, \lambda'} \left(\hat{b}_{\mathbf{q}, \sigma} e^{i\Omega_{\mathbf{q}} t} + \hat{b}_{\mathbf{q}, \sigma}^\dagger e^{-i\Omega_{\mathbf{q}} t} \right) \right] \quad (7)$$

where $\Omega_{\mathbf{q}} = \omega_{\mathbf{q}}(1 - \hat{\mathbf{k}} \cdot \hat{\mathbf{q}})$ and $g_{\mathbf{k},\hat{\mathbf{q}}}^{\sigma,\lambda,\lambda'} = \left(\varepsilon_{(\hat{\mathbf{k}},\lambda)}^i \varepsilon_{(\hat{\mathbf{k}},\lambda')}^i + (\hat{\mathbf{k}} \times \varepsilon_{(\hat{\mathbf{k}},\lambda)})^i (\hat{\mathbf{k}} \times \varepsilon_{(\hat{\mathbf{k}},\lambda')})^j \right) \varepsilon_{ij}^{(\hat{\mathbf{q}},\sigma)}$ is the geometric factor. Equation (7) is obtained by summing over \mathbf{k}' where delta function $\delta(\mathbf{k} - \mathbf{k}' \pm \mathbf{q})$ is involved for each terms, which gives, $\omega_{\mathbf{k}} - \omega_{\mathbf{k}'} = \pm \omega_{\mathbf{q}}$ and then using $\omega_{\mathbf{k}} - \omega_{\mathbf{k}'} \approx \mp \omega_{\mathbf{q}} \hat{\mathbf{k}} \cdot \hat{\mathbf{q}}$ (details in Appendix A). This interaction reveals a *graviton-photon energy exchange*. Just as in Raman spectroscopy, where photons undergo inelastic scattering with molecular vibrations (Stokes and anti-Stokes lines), here the photon gains or loses energy by absorbing or emitting a graviton. For GW detection, where $\omega_{\mathbf{k}} \gg \omega_{\mathbf{q}}$, this manifests as frequency shift, which as we show below can be treated as an accumulative phase $\phi_{\mathbf{k}}(t)$.

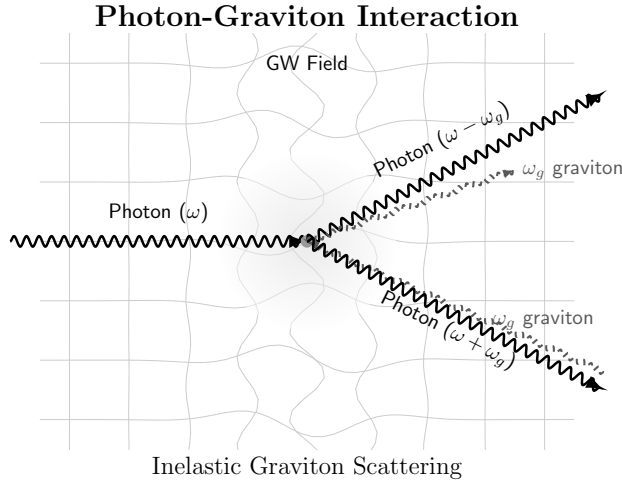


FIG. 1: Schematic diagram of the inelastic graviton scattering.

To study the effect of graviton-photon interaction, as depicted in Fig. (1), we assume the initial state to be a product state $\hat{\rho}(0) = \hat{\rho}_{\text{ph}}(0) \otimes \hat{\rho}_{\text{gw}}(0)$. By evaluating time-evolution operator $U_I(t)$ and tracing out the graviton field (assumed to be in a coherent state $|\beta\rangle$), we arrive at the reduced photon density matrix (details in Appendix B):

$$\hat{\rho}_{\text{ph}}(t) = \sum_{n,n'} \rho_{nn'} |n\rangle \langle n'| e^{2i \text{Im}\{\sum_{\mathbf{q}} (\tilde{\alpha}_n - \tilde{\alpha}_{n'}) \beta_{\mathbf{q}}^*\}} e^{-\frac{1}{2} |\tilde{\alpha}_n - \tilde{\alpha}_{n'}|^2} \quad (8)$$

The above equation is central to our analysis and we emphasize the following key aspects: First, the term $2i \text{Im}\{\sum_{\mathbf{q}} (\tilde{\alpha}_{\mathbf{q},n} - \tilde{\alpha}_{\mathbf{q},n'}^*) \beta_{\mathbf{q}}^*\}$ is purely imaginary and hence leads to the additional phase in photons due to its interaction with gravitons. Consequently, it is clear from Eq. (8) that the photon state $|n\rangle$ evolves in time as, $|n\rangle \rightarrow e^{2i \text{Im}\{\sum_{\mathbf{q}} \tilde{\alpha}_{\mathbf{q},n}^* \beta_{\mathbf{q}}^*\}} |n\rangle$. Second, the exponential decay factor given by $e^{-\frac{1}{2} |\tilde{\alpha}_n - \tilde{\alpha}_{n'}|^2}$ represents gravitational decoherence. This term arises because the interaction creates entanglement between the photons and the

graviton environment. If the graviton ‘‘measures’’ which path the photon took (by picking up a distinct state $\tilde{\alpha}$), the photon’s quantum coherence is suppressed. In the weak-field limit, the coupling constant (contained in $\tilde{\alpha}$) is extremely small. Hence, the information about the path is negligible ($|\tilde{\alpha}|^2 \ll 1$), meaning the decay factor is approximately unity, and the evolution remains unitary for all practical purposes.

III. EMERGENCE OF THE CLASSICAL PHASE

To connect our quantum scattering formalism with standard GW literature [5], we consider the limit of a coherent macroscopic GW. We approximate the graviton field state $|\beta\rangle$ by a coherent amplitude sharply peaked at the GW frequency ω_{gw} , such that $\beta_{\mathbf{q}}^{(\sigma)}/\sqrt{\omega_{\mathbf{q}}} \approx h_0^{(\sigma)} \delta(\omega_{\mathbf{q}} - \omega_{\text{gw}})$. In the single-photon sector relevant to our interference scheme ($|n_{\mathbf{k}} = 1\rangle$), the evolution is fully characterized by the phase acquired by the creation operator, $a_{\mathbf{k}}^\dagger \rightarrow a_{\mathbf{k}}^\dagger e^{i\phi_{\mathbf{k}}(t)}$, where:

$$\phi_{\mathbf{k}}(t) = \frac{1}{2} \text{Im} \left\{ \sum_{\lambda, \lambda'} \frac{\omega_{\mathbf{k}} g_{\hat{\mathbf{k}}, \text{gw}}^{\sigma, \lambda, \lambda'}}{\Omega_{\text{gw}}} (1 - e^{-i\Omega_{\text{gw}}t}) h_0^{(\sigma)} \right\}, \quad (9)$$

and $\Omega_{\text{gw}} = \omega_{\text{gw}}(1 - \hat{\mathbf{k}} \cdot \hat{\mathbf{q}})$. We identify the term $(1 - e^{-i\Omega_{\text{gw}}t})/\Omega_{\text{gw}}$ as the time integral of the interaction phase factor $-i \int_0^t dt' e^{-i\Omega_{\text{gw}}t'}$. This allows us to recast the accumulated phase into a form directly comparable to classical interferometry [5, 7]:

$$\phi_{\mathbf{k}}(t) = -\omega_{\mathbf{k}} \left(\frac{1}{2} \int_0^t dt' h_{\text{eff}}(t') \right). \quad (10)$$

Here, $h_{\text{eff}}(t) = g_{\hat{\mathbf{k}}, \hat{\mathbf{q}}}^{\sigma, \lambda, \lambda'} e^{-i\Omega_{\mathbf{q}}t} h_0^{(\sigma)}$ encapsulates the geometric projection of the metric perturbation onto the photon polarization basis, recovering the standard antenna pattern functions derived in classical general relativity [7].

Equation (10) is the first key result of this work. It demonstrates that the accumulated quantum phase shift arising from graviton-photon scattering is mathematically identical to the phase shift induced by variations in optical path length in the classical description. In observatories like LIGO-VIRGO-KAGRA [19–21], this phase is operationally interpreted as a time delay $\Delta\tau = \phi_{\mathbf{k}}/\omega_{\mathbf{k}}$. Our derivation reveals that this *time delay* can be explained as a cumulative record of inelastic energy exchanges between the photons and gravitons. While consistent in the classical limit, this field-theoretic perspective is essential for describing

interferometers where the quantum state of light (e.g., entanglement or squeezing) plays a non-trivial role in the detection statistics [22–24].

Having established that the interaction between gravitons and photons induces a frequency shift, effectively manifesting as a phase accumulation or time delay in the photon propagation, a detection scheme sensitive to such frequency-dependent phase shifts is required to observe this effect. In the rest of this work, we propose using Hong-Ou-Mandel (HOM) interference [16], a two-photon quantum phenomenon, as the probe.

IV. GW-INDUCED HOM INTERFERENCE

In the standard HOM experiment, the indistinguishability of photons at a beam splitter dictates their bunching behavior. Our proposal leverages the fact that the GW-induced phase shift $\phi_{\mathbf{k}}(t)$ (Eq. (9)) acts as a distinguishing marker. This *gravitational distinguishability* modifies the quantum interference pattern, converting the graviton-photon interaction into a measurable change in coincidence counts.

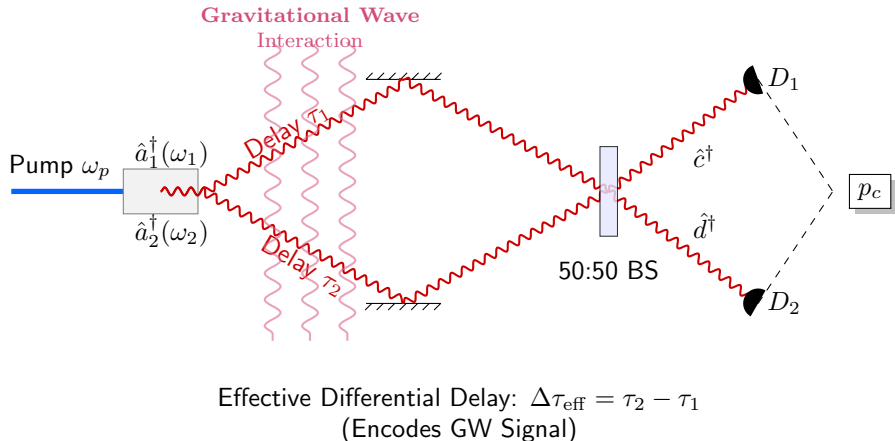


FIG. 2: Schematic diagram of effective differential time delay in the HOM-type experiment.

To go about this, we first formally describe the HOM interference pattern in the presence of GW-induced time delays. We consider the general case of frequency-entangled photons generated, for instance, by spontaneous parametric down-conversion (SPDC)[25] pumped by a monochromatic beam of frequency ω_p . The signal and idler photons satisfy energy conservation. As shown in Fig. (2), the quantum state of the photon pair entering the

interferometer is described by the joint spectral amplitude (JSA), $f(\omega_1, \omega_2)$:

$$|\Psi\rangle_{\text{in}} = \int d\omega_1 d\omega_2 f(\omega_1, \omega_2) \hat{a}_1^\dagger(\omega_1) \hat{a}_2^\dagger(\omega_2) |0\rangle_{1,2} , \quad (11)$$

where \hat{a}_1^\dagger and \hat{a}_2^\dagger create photons in the spatial modes a and b (the two interferometer arms), and the state is normalized such that $\int d\omega_1 d\omega_2 |f(\omega_1, \omega_2)|^2 = 1$.

As the photons traverse the arms, the graviton-photon interaction induces effective time delays τ_1 and τ_2 in the respective arms (see Eq. (10)). This imposes a frequency-dependent phase shift on the creation operators: $\hat{a}_1^\dagger(\omega) \rightarrow \hat{a}_1^\dagger(\omega)e^{-i\omega\tau_1}$ and $\hat{a}_2^\dagger(\omega) \rightarrow \hat{a}_2^\dagger(\omega)e^{-i\omega\tau_2}$. The state arriving at the beam splitter is then:

$$|\Psi'\rangle_{\text{in}} = \int d\omega_1 d\omega_2 f(\omega_1, \omega_2) e^{-i(\omega_1\tau_1 + \omega_2\tau_2)} \hat{a}_1^\dagger(\omega_1) \hat{a}_2^\dagger(\omega_2) |0\rangle_{1,2} . \quad (12)$$

As shown in Fig. (2), the 50:50 beam splitter mixes the modes \hat{a}_1 and \hat{a}_2 into output modes \hat{c} and \hat{d} via the transformations $\hat{a}_1^\dagger \rightarrow (\hat{c}^\dagger + \hat{d}^\dagger)/\sqrt{2}$ and $\hat{a}_2^\dagger \rightarrow (\hat{c}^\dagger - \hat{d}^\dagger)/\sqrt{2}$. Substituting these into the state vector, the output state $|\Psi\rangle_{\text{out}}$ becomes:

$$|\Psi\rangle_{\text{out}} = \frac{1}{2} \int d\omega_1 d\omega_2 f(\omega_1, \omega_2) e^{-i(\omega_1\tau_1 + \omega_2\tau_2)} \left(\hat{c}^\dagger(\omega_1) \hat{c}^\dagger(\omega_2) - \hat{d}^\dagger(\omega_1) \hat{d}^\dagger(\omega_2) - \hat{c}^\dagger(\omega_1) \hat{d}^\dagger(\omega_2) + \hat{c}^\dagger(\omega_2) \hat{d}^\dagger(\omega_1) \right) |0\rangle \quad (13)$$

The observable of interest is the probability of a coincidence detection, p_c , where one photon is detected in port D_1 and one in port D_2 . This corresponds to the projection onto the subspace spanned by $\hat{c}^\dagger \hat{d}^\dagger$. The probability $p_c = \langle \Psi |_{\text{out}} \hat{\Pi}_{cd} | \Psi \rangle_{\text{out}}$ is calculated as:

$$p_c = \frac{1}{2} - \frac{1}{4} \int d\omega_1 d\omega_2 [f^*(\omega_2, \omega_1) f(\omega_1, \omega_2) e^{-i\Delta\omega\Delta\tau_{\text{eff}}} + \text{c.c.}] , \quad (14)$$

where $\Delta\omega = \omega_2 - \omega_1$ and $\Delta\tau_{\text{eff}} = \tau_2 - \tau_1$ is the effective differential time delay induced by the GW.

Equation (14) describes the famous HOM dip. When $\Delta\tau_{\text{eff}} = 0$, the interference term is maximized, and for a symmetric JSA ($f(\omega_1, \omega_2) = f(\omega_2, \omega_1)$), the coincidence probability drops to zero ($p_c \rightarrow 0$). The GW signal $\Delta\tau_{\text{eff}}(t)$ modulates this probability, encoding the graviton interaction into the coincidence rate.

To detect the minute variations in $\Delta\tau_{\text{eff}}$ caused by gravitons, we must optimize the working point of the interferometer. We assume a Gaussian spectral distribution for the photons with bandwidth σ . For unentangled identical photons, or entangled photons with symmetric Gaussian joint spectra, the coincidence probability simplifies to:

$$p_c(\Delta\tau) = \left(1 - e^{-\sigma^2 \Delta\tau^2} \right) / 2 , \quad (15)$$

where $\Delta\tau$ is the total path length difference. For a pure GW signal, $\Delta\tau = \Delta\tau_{\text{eff}} \propto h_0$. Expanding around zero delay:

$$p_c \approx \sigma^2 \Delta\tau_{\text{eff}}^2 / 2 + \mathcal{O}(\Delta\tau_{\text{eff}}^4) . \quad (16)$$

This reveals a quadratic dependence on the strain h_0 , which vanishes to first order. This

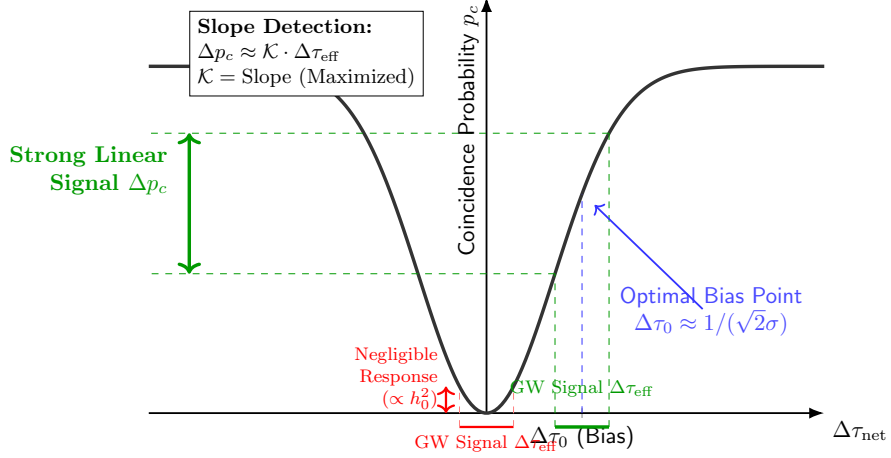


FIG. 3: Illustration of the slope detection vs. quadratic detection.

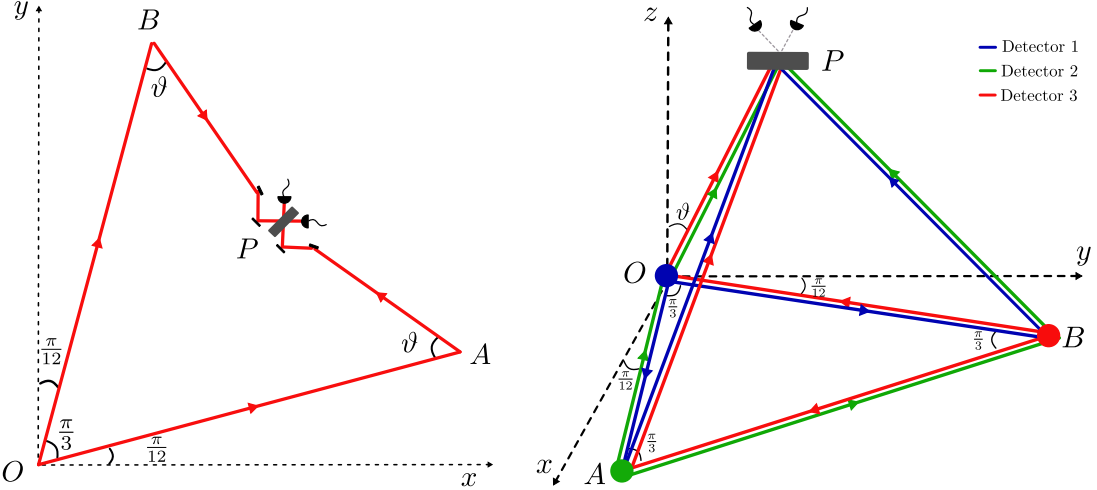


FIG. 4: Possible geometrical configurations in 2D and 3D for HOM based GW detectors.

"dark port" problem is analogous to detecting at the bottom of a fringe in a classical Michelson interferometer [5]; the sensitivity to small displacements is zero at the extremum. To achieve *linear sensitivity* to h_0 , we must bias the interferometer away from the perfect dip. We introduce a static, controlled time delay $\Delta\tau_0$ such that the net delay is

$\Delta\tau_{\text{net}} = \Delta\tau_0 + \Delta\tau_{\text{eff}}(t)$. Expanding the coincidence probability around this bias point:

$$\begin{aligned} p_{\text{net}} &\approx p_c(\Delta\tau_0) + \left. \frac{dp_c}{d\tau} \right|_{\tau_0} \Delta\tau_{\text{eff}} \\ &= \frac{1}{2} \left(1 - e^{-\sigma^2 \Delta\tau_0^2} \right) + \left(\sigma^2 \Delta\tau_0 e^{-\sigma^2 \Delta\tau_0^2} \right) \Delta\tau_{\text{eff}}(t) + \mathcal{O}(h_0^2). \end{aligned} \quad (17)$$

The signal is now the time-varying fluctuation in the coincidence rate, $\Delta p_c(t)$, which is linearly proportional to the effective delay:

$$\Delta p_c(t) \approx \mathcal{K}(\sigma, \Delta\tau_0) \Delta\tau_{\text{eff}}(t), \quad (18)$$

where, as shown in Fig. (3), the sensitivity factor $\mathcal{K} = \sigma^2 \Delta\tau_0 e^{-\sigma^2 \Delta\tau_0^2}$ is maximized when $\Delta\tau_0 = 1/(\sqrt{2}\sigma)$. The total number of coincidence counts N_c measured over a time T is $N_c = \Gamma \int_0^T p_{\text{net}}(t) dt$, where Γ is the photon flux. The gravitational wave signal is extracted from the fluctuations in these counts:

$$\delta N_c = \Gamma \mathcal{K} \int_0^T \Delta\tau_{\text{eff}}(t) dt. \quad (19)$$

This result demonstrates that by monitoring the variations in photon coincidence rates at the slope of the HOM dip, one can directly measure the phase shifts induced by the graviton-photon scattering.

V. GEOMETRICAL CONFIGURATIONS AND ANGULAR RESPONSE

To evaluate the detector's sensitivity to GWs from different sky locations, we calculate the accumulated effective time delay Δt for specific interferometer geometries. Using the scattering phase derived in Eq. (10), the delay for a photon propagating along a unit vector $\hat{\mathbf{k}}$ over a path length L is given by the projection of the metric perturbation h_{ij} along the optical trajectory [7]:

$$c\Delta t \approx L + \frac{1}{2} \hat{k}^i \hat{k}^j \int_{t_0}^{t_0+L/c} dt h_{ij}(t, \mathbf{x}(t)). \quad (20)$$

We propose two distinct configurations to exploit this response:

1. **2D Planar Setup:** We first consider a symmetric planar configuration suitable for ground-based implementation, as shown in left side of Fig. (4). In the long-wavelength limit ($\omega_{\text{gw}} L/c \ll 1$), the differential time delay simplifies to:

$$c\Delta\tau_{\text{eff}} \approx \mathcal{C}_{\text{2D}} L (h_{xx} - h_{yy}), \quad (21)$$

where \mathcal{C}_{2D} is a geometric factor of order unity. This recovers the standard quadrupolar antenna pattern characteristic of current terrestrial observatories (e.g., LIGO), with maximum sensitivity to $+$ polarization and zero response to \times polarization aligned with the axes.

2. **3D Pyramidal Setup:** For space-based missions, we propose a three-dimensional pyramidal configuration (see right side of the Fig. (4)) consisting of three non-coplanar interferometers sharing a common vertex [26–29]. Unlike planar detectors, this geometry couples to off-diagonal metric components in the detector frame. The differential response for one such interferometer (Detector 1) includes terms such as:

$$\left. \frac{c \Delta \tau_{\text{eff}}}{L} \right|_{D_1} = \frac{1}{4} (h_{xx} + h_{yy}) + \frac{3\sqrt{3}}{4} (h_{xx} - h_{yy}) + \sqrt{\frac{3}{2}} (h_{yz} - h_{xz}) + \frac{1}{2} h_{xy} , \quad (22)$$

where L is the characteristic arm length. As detailed in Appendix C, this sensitivity to h_{xz} and h_{yz} components provides a significantly more isotropic antenna pattern, reducing blind spots and improving source localization capabilities compared to a single planar detector.

VI. 3D SENSITIVITY AND EXPERIMENTAL OUTLOOK

The specific coupling to off-diagonal metric components (h_{xz}, h_{yz}) shown in Eq. (22) represents a significant deviation from the response of planar interferometers. In standard configurations like LIGO or LISA, the detector response is maximized for GWs propagating perpendicular to the detector plane, while vanishing for waves incident along the arm bisectors (blind spots). As illustrated in Fig. (5), each individual interferometer in our proposed 3D pyramidal configuration possesses a distinct antenna pattern. Crucially, the orientation of these patterns is mutually complementary. When operating as a network, the combined response — averaged over three detectors — approximates a monopole-like sensitivity (Fig. (6)). This quasi-isotropic coverage ensures that there are no blind spots on the sky, enabling continuous monitoring of transient sources regardless of their sky location. Furthermore, the simultaneous measurement of distinct linear combinations of the strain tensor components (h_{ij}) by the three detectors breaks the degeneracy typically found

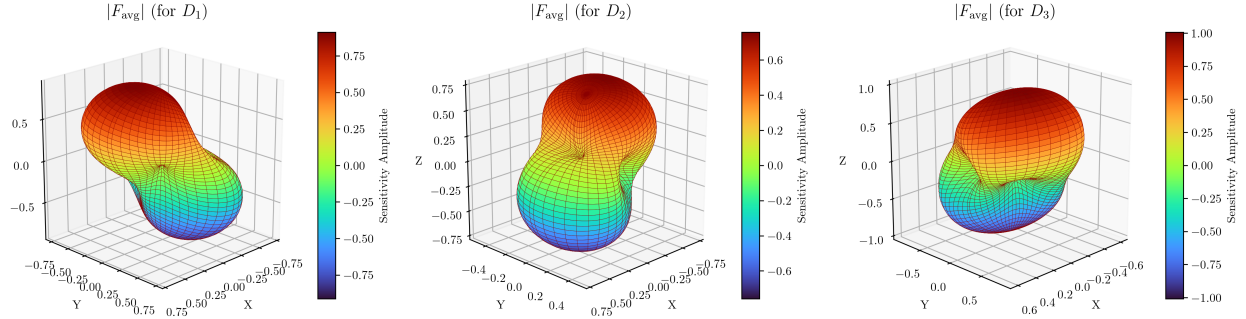


FIG. 5: Directional sensitivity (antenna patterns) for the three individual detectors in the pyramidal configuration ($\vartheta = \pi/6$). Unlike planar detectors which share common null directions, the 3D geometry ensures that the maxima of one detector cover the minima of the others.

in single-detector observations, significantly enhancing the capability for source localization and polarization resolution.

While the theoretical sensitivity of this HOM-based scheme is promising, we acknowledge that a ground-based implementation faces significant challenges. The requisite phase stability and photon path-length control are stringent, and seismic noise may mask the subtle quantum interference effects at low frequencies. However, the architecture is naturally suited for a space-based mission. In the vacuum of space, long baselines can be achieved without scattering losses, and the drag-free control technologies developed for LISA could stabilize the spacecraft formation to the requisite precision. In such an environment, the quantum advantages of this counting experiment—specifically its robustness against laser intensity noise compared to classical fringe locking—could offer a complementary observational window for the gravitational universe.

Finally, it is instructive to distinguish the present framework from the seminal analysis of quantum mechanical noise in interferometers by Caves [30]. Caves' formalism focuses on the fundamental limits of measurement precision, demonstrating that the shot-noise limit in a classical interferometer arises from vacuum fluctuations entering the unused port, and can be surpassed using squeezed states. However, in Caves' analysis, the GW is treated as a classical tidal force that modifies the boundary conditions (mirror positions) of the EM field modes. In contrast, our work addresses the microscopic origin of the signal itself. By treating the interaction as a scattering process between the quantized EM and gravita-

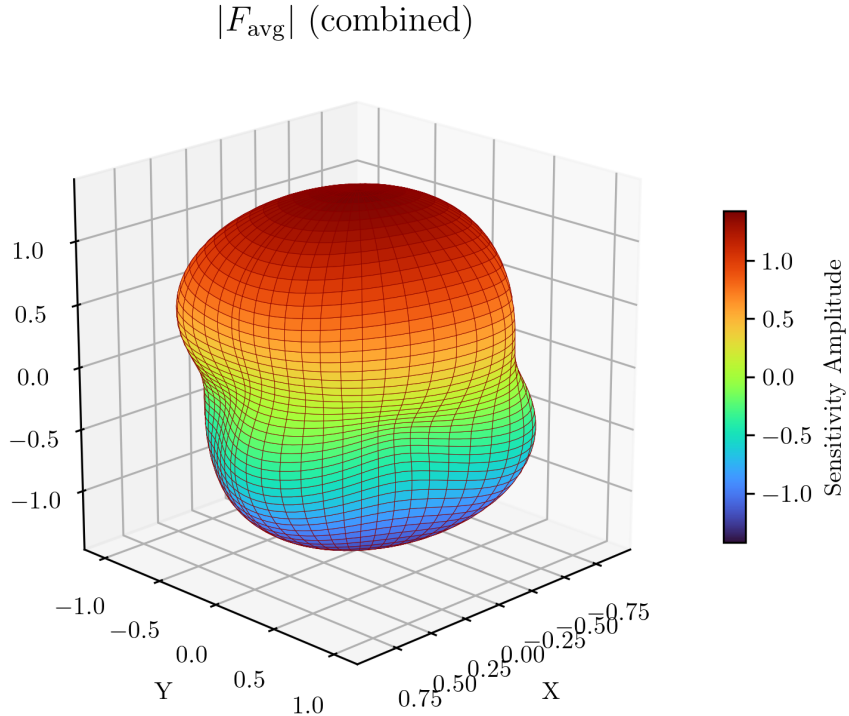


FIG. 6: The combined angular sensitivity of the 3D network ($\vartheta = \pi/6$), calculated as the root-mean-square response of the three component interferometers. The resulting pattern is nearly isotropic, demonstrating full-sky coverage without significant blind spots.

tional fields, we derive the accumulated phase not as a geometric boundary effect, but as a consequence of inelastic energy exchange. Furthermore, while Caves' analysis pertains to intensity measurements (first-order coherence, $g^{(1)}$), our proposed detection scheme relies on HOM interference (second-order coherence, $g^{(2)}$). This shifts the measurement basis from field amplitude quadratures to photon distinguishability, offering a complementary modality that may be less susceptible to specific classes of low-frequency laser noise.

Acknowledgement: The authors are grateful to A. Chowdhury, I. Chakraborty, P. G. Christopher, S. Mondal, and T. Parvez for their valuable discussions and feedback on the earlier draft. The work is supported by SERB-CRG/2022/002348.

Appendix A: Photon-Graviton induced phase evolution

In this section, we derive the effective photon dynamics induced by the interaction with gravitons. We work in the interaction picture, treating the gravitational wave as a quantized perturbation, and show explicitly how the effective phase evolution of photon creation operators emerges from the scattering dynamics.

1. Interaction Hamiltonian

The total Hamiltonian of the photon-graviton system can be written as

$$H = H_{\text{ph}} + H_{\text{GW}} + H_{\text{int}}. \quad (\text{A1})$$

The free electromagnetic Hamiltonian of the photons is

$$H_{\text{ph}} = \sum_{\mathbf{k}, \lambda} \hbar \omega_{\mathbf{k}} a_{\mathbf{k}, \lambda}^\dagger a_{\mathbf{k}, \lambda}, \quad (\text{A2})$$

where $a_{\mathbf{k}, \lambda}$ annihilates a photon of wave vector \mathbf{k} , polarization λ , and frequency $\omega_{\mathbf{k}} = |\mathbf{k}|$ (we adopt natural units $\hbar = c = 1$ henceforth, restoring them only for final observables). The free graviton Hamiltonian is

$$H_{\text{GW}} = \sum_{\mathbf{q}, \sigma} \hbar \omega_{\mathbf{q}} b_{\mathbf{q}, \sigma}^\dagger b_{\mathbf{q}, \sigma}, \quad (\text{A3})$$

To explicitly define the field expansions, we must fix the gauge. We adopt the *Transverse-Traceless (TT) gauge* for the gravitational field ($h_{0\mu} = 0$, $h_i^i = 0$, $\partial^j h_{ij} = 0$) and the *Coulomb gauge* for the electromagnetic field ($A^0 = 0$, $\nabla \cdot \mathbf{A} = 0$). In the TT gauge, the quantized metric perturbation is:

$$h_{ij}(\mathbf{x}, t) = \sum_{\mathbf{q}, \sigma} \frac{1}{\sqrt{2\omega_{\mathbf{q}}(2\pi)^3}} \left[b_{\mathbf{q}, \sigma} e^{i(\mathbf{q} \cdot \mathbf{x} - \omega_{\mathbf{q}} t)} + b_{\mathbf{q}, \sigma}^\dagger e^{-i(\mathbf{q} \cdot \mathbf{x} - \omega_{\mathbf{q}} t)} \right] \varepsilon_{ij}^{(\mathbf{q}, \sigma)}. \quad (\text{A4})$$

where $b_{\mathbf{q}, \sigma}$ annihilates a graviton with polarization σ . Similarly, in the Coulomb gauge, the vector potential is:

$$A^i(\mathbf{x}, t) = \sum_{\mathbf{k}, \lambda} \frac{1}{\sqrt{2\omega_{\mathbf{k}}(2\pi)^3}} \left[a_{\mathbf{k}, \lambda} e^{i(\mathbf{k} \cdot \mathbf{x} - \omega_{\mathbf{k}} t)} \right]$$

$$+ a_{\mathbf{k},\lambda}^\dagger e^{-i(\mathbf{k}\cdot\mathbf{x}-\omega_{\mathbf{k}}t)} \Big] \varepsilon_i^{(\mathbf{k},\lambda)} , \quad (\text{A5})$$

The interaction Hamiltonian arises from the minimal coupling of the metric perturbation to the electromagnetic stress-energy tensor T_{EM}^{ij} :

$$H_{\text{int}} = \frac{1}{2} \int d^3x \, h_{ij}(\mathbf{x}, t) T_{\text{EM}}^{ij}(\mathbf{x}, t) , \quad (\text{A6})$$

where T_{EM}^{ij} is the spatial part of the stress-energy tensor of the EM field given by,

$$T_{\text{EM}}^{ij} = \left(F^{i\mu} F_\mu^j - \frac{1}{4} \delta^{ij} F_{\mu\nu} F^{\mu\nu} \right) . \quad (\text{A7})$$

Since h_{ij} is traceless in the TT gauge ($h_{ij}\delta^{ij} = 0$), the second term vanishes. Furthermore, in the Coulomb gauge ($E^i = -\dot{A}^i, B^k = \epsilon^{kij}\partial_i A_j$), the contraction simplifies to $h_{ij}T_{\text{EM}}^{ij} = h_{ij}(E^i E^j + B^i B^j)$.

$$H_{\text{int}} = \frac{1}{2} \sum_{\mathbf{k}, \mathbf{k}', \mathbf{q}} \sum_{\sigma, \lambda, \lambda'} \frac{\sqrt{\omega_{\mathbf{k}} \omega_{\mathbf{k}'}}}{2(2\pi)^{3/2} \sqrt{\omega_{\mathbf{q}}}} g_{\mathbf{k}, \mathbf{k}', \mathbf{q}}^{\sigma, \lambda, \lambda'} \times \left[a_{\mathbf{k}, \lambda}^\dagger a_{\mathbf{k}', \lambda'} b_{\mathbf{q}, \sigma} e^{-i(\omega_{\mathbf{k}} - \omega_{\mathbf{k}'} - \omega_{\mathbf{q}})t} \delta^3(\mathbf{k} - \mathbf{k}' - \mathbf{q}) \right. \\ \left. + a_{\mathbf{k}, \lambda}^\dagger a_{\mathbf{k}', \lambda'} b_{\mathbf{q}, \sigma}^\dagger e^{-i(\omega_{\mathbf{k}} - \omega_{\mathbf{k}'} + \omega_{\mathbf{q}})t} \delta^3(\mathbf{k} - \mathbf{k}' + \mathbf{q}) \right] , \quad (\text{A8})$$

where, $g_{\hat{\mathbf{k}}, \hat{\mathbf{k}'}, \hat{\mathbf{q}}}^{\sigma, \lambda, \lambda'} = \left(\varepsilon_{(\hat{\mathbf{k}}, \lambda)}^i \varepsilon_{(\hat{\mathbf{k}'}, \lambda')}^j + (\hat{\mathbf{k}} \times \varepsilon_{(\hat{\mathbf{k}}, \lambda)})^i (\hat{\mathbf{k}} \times \varepsilon_{(\hat{\mathbf{k}'}, \lambda')})^j \right) \varepsilon_{ij}^{(\hat{\mathbf{q}}, \sigma)}$ is the geometric polarization factor. The momentum-conserving delta functions imply an energy resonance condition $\omega_{\mathbf{k}} - \omega_{\mathbf{k}'} = \pm \omega_{\mathbf{q}}$. This describes an *inelastic scattering process* where the photon gains or loses energy $\hbar\omega_{\mathbf{q}}$ by absorbing or emitting a graviton. This mechanism is formally analogous to the Stokes (emission) and anti-Stokes (absorption) shifts in Raman spectroscopy, where the gravitational wave acts as a pump field modulating the photon energy [15]. We will see that in our proposal using quantum interference this energy exchange (graviton absorption or emission) will cause frequency shift of photons leading to an additional phase for the photons in the interferometric experiment.

For gravitational waves of astrophysical interest, $\omega_{\mathbf{q}} \ll \omega_{\mathbf{k}}$. Consequently, the scattering is quasi-elastic: the photon direction is largely preserved ($\hat{\mathbf{k}} \approx \hat{\mathbf{k}'}$), and the frequency shift is small. Using the approximation $\omega_{\mathbf{k}} - \omega_{\mathbf{k}'} \approx \omega_{\mathbf{k}} - |\mathbf{k} \mp \mathbf{q}| \approx \pm \mathbf{q} \cdot \hat{\mathbf{k}}$, the phase arguments simplify to:

$$(\omega_{\mathbf{k}} - \omega_{\mathbf{k}'} \mp \omega_{\mathbf{q}})t \approx \mp \omega_{\mathbf{q}}(1 - \hat{\mathbf{k}} \cdot \hat{\mathbf{q}})t \equiv \mp \Omega_{\mathbf{q}}t . \quad (\text{A9})$$

The effective interaction Hamiltonian governing the phase evolution is then:

$$H_{\text{int}} \approx \frac{1}{2} \sum_{\mathbf{k}, \mathbf{q}} \sum_{\sigma, \lambda, \lambda'} \frac{\omega_{\mathbf{k}}}{2(2\pi)^{3/2} \sqrt{\omega_{\mathbf{q}}}} g_{\hat{\mathbf{k}}, \hat{\mathbf{q}}}^{\sigma, \lambda, \lambda'} \times [\hat{n}_{\mathbf{k}, \lambda \lambda'} (b_{\mathbf{q}, \sigma} e^{i\Omega_{\mathbf{q}} t} + b_{\mathbf{q}, \sigma}^\dagger e^{-i\Omega_{\mathbf{q}} t})] , \quad (\text{A10})$$

where $\hat{n}_{\mathbf{k}, \lambda \lambda'} = a_{\mathbf{k}, \lambda}^\dagger a_{\mathbf{k}, \lambda'}$ is the photon number density operator in the polarization basis and $\Omega_{\mathbf{q}} = \omega_{\mathbf{q}} (1 - \hat{\mathbf{k}} \cdot \hat{\mathbf{q}})$.

Appendix B: Time evolution of photon density matrix

We consider the density matrix of the total system, initialized as a product state of the photon and graviton sectors:

$$\hat{\rho}(0) = \hat{\rho}_{\text{ph}}(0) \otimes \hat{\rho}_{\text{gw}}(0) . \quad (\text{B1})$$

The photon state is general, $\hat{\rho}_{\text{ph}} = \sum_{n, n'} \rho_{nn'} |n\rangle \langle n'|$, where $|n\rangle$ represents a Fock state of the relevant optical mode. The unitary time evolution in the interaction picture is given by the time-ordered exponential:

$$U_I(t) = \mathcal{T} \exp \left(-i \int_0^t dt' H_{\text{int}}(t') \right) . \quad (\text{B2})$$

Using the Magnus expansion up to second order, this can be written as:

$$U_I(t) = \exp \left(-i \int_0^t dt' H_{\text{int}}(t') - \frac{1}{2} \int_0^t dt' \int_0^{t'} dt'' [H_{\text{int}}(t'), H_{\text{int}}(t'')] \right) . \quad (\text{B3})$$

The first-order term is linear in graviton operators $(\hat{b}, \hat{b}^\dagger)$ and drives the displacement of the gravitational field:

$$-i \int_0^t dt' H_{\text{int}}(t') = \sum_{\mathbf{k}, \mathbf{q}} \sum_{\sigma, \lambda, \lambda'} \frac{\omega_{\mathbf{k}}}{2(2\pi)^3 \sqrt{2\omega_{\mathbf{q}}}} \hat{n}_{\mathbf{k}, \lambda, \lambda'} \left[\hat{b}_{\mathbf{q}, \sigma}^\dagger \alpha_{\mathbf{k}, \mathbf{q}}^{\sigma, \lambda, \lambda'}(t) - \hat{b}_{\mathbf{q}, \sigma} \left(\alpha_{\mathbf{k}, \mathbf{q}}^{\sigma, \lambda, \lambda'}(t) \right)^* \right] , \quad (\text{B4})$$

where we have defined the time-dependent coupling coefficient:

$$\alpha_{\mathbf{k}, \mathbf{q}}^{\sigma, \lambda, \lambda'}(t) = g_{\hat{\mathbf{k}}, \hat{\mathbf{q}}}^{\sigma, \lambda, \lambda'} \left(\frac{1 - e^{-i\Omega_{\mathbf{q}} t}}{\Omega_{\mathbf{q}}} \right) = i g_{\hat{\mathbf{k}}, \hat{\mathbf{q}}}^{\sigma, \lambda, \lambda'} \int_0^t dt' e^{-i\Omega_{\mathbf{q}} t'} . \quad (\text{B5})$$

The second-order term involves the commutator $[H_{\text{int}}(t'), H_{\text{int}}(t'')]$, which reduces to the c-number commutator $[\hat{b}_{\mathbf{q}}, \hat{b}_{\mathbf{q}'}^\dagger] = \delta_{\mathbf{q}\mathbf{q}'}$. This term contributes only a global phase factor $\Phi(t)$

(a c-number in the graviton subspace, though diagonal in the photon number basis), and all higher-order commutators vanish. The total evolution operator can thus be factorized as:

$$U_I(t) = e^{i\Phi(t)} \prod_{\mathbf{q},\sigma} \hat{D}_{\mathbf{q}}(\tilde{\alpha}_{\mathbf{q}}^\sigma) , \quad (\text{B6})$$

where $\hat{D}_{\mathbf{q}}(\gamma) = \exp\left(\gamma \hat{b}_{\mathbf{q}}^\dagger - \gamma^* \hat{b}_{\mathbf{q}}\right)$ is the displacement operator acting on the graviton field, and the displacement amplitude depends on the photon number operator:

$$\tilde{\alpha}_{\mathbf{q}}^\sigma = \sum_{\mathbf{k},\lambda,\lambda'} \frac{\omega_{\mathbf{k}}}{2(2\pi)^3 \sqrt{2\omega_{\mathbf{q}}}} \hat{n}_{\mathbf{k},\lambda,\lambda'} \alpha_{\mathbf{k},\mathbf{q}}^{\sigma,\lambda,\lambda'}(t) . \quad (\text{B7})$$

1. Reduced Photon Dynamics

We now evolve the total density matrix $\hat{\rho}(t) = U_I(t)[\hat{\rho}_{\text{ph}} \otimes \hat{\rho}_{\text{gw}}]U_I^\dagger(t)$. We assume the gravitational wave background is described by a coherent state $|\beta\rangle_{\text{gw}}$ (classical GW approximation), so $\hat{\rho}_{\text{gw}} = |\beta\rangle\langle\beta|$. The photon state is expanded in the number basis $|n\rangle$. Since the operator $\hat{\tilde{\alpha}}$ is diagonal in the photon number basis, let $\tilde{\alpha}_n$ denote its eigenvalue for the state $|n\rangle$. The evolved state is:

$$\begin{aligned} \hat{\rho}(t) &= \sum_{n,n'} \rho_{nn'} |n\rangle\langle n'| \otimes \hat{D}(\tilde{\alpha}_n) |\beta\rangle\langle\beta| \hat{D}^\dagger(\tilde{\alpha}_{n'}) \\ &= \sum_{n,n'} \rho_{nn'} |n\rangle\langle n'| \otimes e^{i\Theta_{nn'}} |\beta + \tilde{\alpha}_n\rangle_{\text{gw}} \langle\beta + \tilde{\alpha}_{n'}|_{\text{gw}} , \end{aligned} \quad (\text{B8})$$

where we used the displacement property $\hat{D}(\alpha) |\beta\rangle = e^{i\text{Im}(\alpha\beta^*)} |\alpha + \beta\rangle$ (up to global phases). The term $\Theta_{nn'}$ collects the phase factors arising from the displacement algebra. To obtain the reduced photon density matrix, we trace out the gravitational degrees of freedom:

$$\begin{aligned} \hat{\rho}_{\text{ph}}(t) &= \text{Tr}_{\text{gw}}[\hat{\rho}(t)] \\ &= \sum_{n,n'} \rho_{nn'} |n\rangle\langle n'| e^{i\Theta_{nn'}} \langle\beta + \tilde{\alpha}_{n'}|\beta + \tilde{\alpha}_n\rangle \\ &= \sum_{n,n'} \rho_{nn'} |n\rangle\langle n'| \underbrace{\exp(i\text{Im}[(\tilde{\alpha}_n - \tilde{\alpha}_{n'})\beta^*])}_{\text{Unitary Phase (Signal)}} \underbrace{\exp\left(-\frac{1}{2}|\tilde{\alpha}_n - \tilde{\alpha}_{n'}|^2\right)}_{\text{Decoherence (Noise)}} . \end{aligned} \quad (\text{B9})$$

The second exponential represents decoherence due to entanglement with the graviton vacuum (spontaneous emission of gravitons), which is negligible for laboratory parameters. The first exponential contains the *gravitational wave signal*.

For a single photon traversing the arm (HOM input state $|1\rangle\langle 1|$ vs vacuum $|0\rangle\langle 0|$), the relative phase accumulated is determined by the term linear in β . Using the approximation $\beta_{\mathbf{q}} \approx \sqrt{2\omega_{\mathbf{q}}} h_0 \delta(\mathbf{q} - \mathbf{q}_{\text{gw}})$, the phase $\phi_{\mathbf{k}}(t)$ acquired by the creation operator $\hat{a}_{\mathbf{k}}^\dagger$ is:

$$\begin{aligned}\phi_{\mathbf{k}}(t) &= \text{Im}(\tilde{\alpha}_{n=1} \beta^*) \\ &= \text{Im} \left[\sum_{\lambda, \lambda'} \frac{\omega_{\mathbf{k}}}{2} g_{\mathbf{k}, \hat{\mathbf{q}}}^{\sigma, \lambda, \lambda'} \left(i \int_0^t dt' e^{-i\Omega_{\mathbf{q}} t'} \right) h_0^{(\sigma)} \right] \\ &= \omega_{\mathbf{k}} \left[\frac{1}{2} \hat{k}^i \hat{k}^j h_0 \varepsilon_{ij} \int_0^t dt' \cos(\Omega_{\mathbf{q}} t') \right].\end{aligned}\quad (\text{B10})$$

This matches the standard expression for the gravitational wave-induced time delay $\Delta t = \frac{1}{2} \int h_{ij} n^i n^j dt$ derived in geometric optics [7]. Thus, our quantum field-theoretical derivation correctly recovers the classical phase shift in the limit of a coherent gravitational wave state, while providing the full density matrix evolution necessary for analyzing quantum interference.

Appendix C: Details of the Proposed Interferometer Configuration

In the previous section, we established that the photon-graviton scattering induces a phase shift on the electromagnetic field mode. For a coherent gravitational wave background, this phase shift can be mapped to an effective variation in the optical path length (or time delay) experienced by the photon. Following the formalism of Ref. [7], the effective time delay Δt for a photon traversing a path of length L with initial position \mathbf{x}_0 at time t_0 is given by:

$$c\Delta t = L + \frac{1}{2} \hat{k}^i \hat{k}^j \int_{t_0}^{t_0+L/c} dt h_{ij}(t, \mathbf{x}_\gamma(t)), \quad (\text{C1})$$

where \hat{k}^i is the unit vector along the photon trajectory, $\mathbf{x}_\gamma(t) = \mathbf{x}_0 + c\hat{\mathbf{k}}(t - t_0)$ is the unperturbed photon path, and h_{ij} is the gravitational wave metric perturbation. For a plane wave propagating along direction $\hat{\mathbf{q}}$ with frequency ω_{gw} , this integrates to:

$$\begin{aligned}c\Delta t &= L + \frac{1}{2} \hat{k}^i \hat{k}^j (h_0 \varepsilon_{ij}) \int_{t_0}^{t_0+L/c} dt \cos \left[\omega_{\text{gw}} \left(t - \hat{\mathbf{q}} \cdot (\mathbf{x}_0 + c\hat{\mathbf{k}}(t - t_0)) / c \right) \right] \\ &= L + \frac{L}{2} \mathcal{F}(k, \varepsilon) \text{sinc} \left(\frac{\omega_{\text{eff}} L}{2c} \right) \cos(\omega_{\text{gw}} t_{\text{mid}} - \Phi_{\text{gw}}),\end{aligned}\quad (\text{C2})$$

where $\mathcal{F}(k, \varepsilon) = \hat{k}^i \hat{k}^j \varepsilon_{ij}$ is the geometric projection factor. We define the effective frequency seen by a photon in a segment with direction $\hat{\mathbf{k}}$ as $\omega_{\text{eff}} = \omega_{\text{gw}}(1 - \hat{\mathbf{q}} \cdot \hat{\mathbf{k}})$.

1. 2D Planar setup

We consider the planar configuration depicted in the main text (Fig. 5). The setup is symmetric about the y -axis. The source is located at the origin O . The photons travel to intermediate mirrors at A and B , and reflect to a final beam splitter at P . The unit vectors for the four optical segments are:

$$\hat{k}_{\text{OA}}^i = \left(\cos \frac{\pi}{12}, \sin \frac{\pi}{12}, 0 \right) \quad (\text{C3a})$$

$$\hat{k}_{\text{AP}}^i = \left(\cos \left(\frac{13\pi}{12} - \vartheta \right), \sin \left(\frac{13\pi}{12} - \vartheta \right), 0 \right) = \left(-\cos \left(\frac{\pi}{12} - \vartheta \right), -\sin \left(\frac{\pi}{12} - \vartheta \right), 0 \right) \quad (\text{C3b})$$

$$\hat{k}_{\text{OB}}^i = \left(\sin \frac{\pi}{12}, \cos \frac{\pi}{12}, 0 \right) \quad (\text{C3c})$$

$$\hat{k}_{\text{BP}}^i = \left(\cos \left(\frac{7\pi}{12} - \vartheta \right), -\sin \left(\frac{7\pi}{12} - \vartheta \right), 0 \right) = \left(-\sin \left(\frac{\pi}{12} - \vartheta \right), -\cos \left(\frac{\pi}{12} - \vartheta \right), 0 \right) \quad (\text{C3d})$$

For arm 1 (OAP), the time taken by a photon to travel the first leg (OA) is:

$$\begin{aligned} c\Delta t_{\text{OA}} &= L + \frac{1}{2} \hat{k}_{\text{OA}}^l \hat{k}_{\text{OA}}^m \overset{\circ}{h}_{lm} \int_{t_0}^{t_0+L/c} \cos[\omega_{\text{gw}}(t - (t - t_0)q_i \hat{k}_{\text{OA}}^i)] \\ &= L + \frac{L}{2} \left(h_{xx} \cos^2 \frac{\pi}{12} + h_{yy} \sin^2 \frac{\pi}{12} + h_{xy} \sin \frac{\pi}{6} \right) \cos(\omega_{\text{gw}} t_0 + \omega_{\text{OA}} L/2) \text{sinc}(\omega_{\text{OA}} L/2) \end{aligned} \quad (\text{C4})$$

where, $\omega_{\text{OA}} = \omega_{\text{gw}} (1 - \cos[\frac{\pi}{12} - \phi] \sin \theta)$. Similarly, using Eq. C2 the remaining time delays can be obtained.

$$c\Delta t_{\text{OB}} = L \left[1 + \frac{1}{2} \left(h_{xx} \sin^2 \frac{\pi}{12} + h_{yy} \cos^2 \frac{\pi}{12} + h_{xy} \sin \frac{\pi}{6} \right) \cos(\omega_{\text{gw}} t_0 + \omega_{\text{OB}} L/2) \text{sinc}(\omega_{\text{OB}} L/2) \right] \quad (\text{C5a})$$

$$\begin{aligned} c\Delta t_{\text{AP}} &= \ell_{\text{AP}} \left[1 + \frac{1}{2} \left(h_{xx} \cos^2 \left(\frac{\pi}{12} - \vartheta \right) + h_{yy} \sin^2 \left(\frac{\pi}{12} - \vartheta \right) + h_{xy} \sin \left(\frac{\pi}{6} - 2\vartheta \right) \right) \right. \\ &\quad \left. \times \text{sinc}(\omega_{\text{AP}} \ell_{\text{AP}}/2) \cos(\omega_{\text{gw}} t_0 + \omega_{\text{AP}} (L + \ell_{\text{AP}}/2)) \right] \end{aligned} \quad (\text{C5b})$$

$$c\Delta t_{\text{BP}} = \ell_{\text{BP}} \left[1 + \frac{1}{2} \left(h_{xx} \sin^2 \left(\frac{\pi}{12} - \vartheta \right) + h_{yy} \cos^2 \left(\frac{\pi}{12} - \vartheta \right) + h_{xy} \sin \left(\frac{\pi}{6} - 2\vartheta \right) \right) \right]$$

$$\times \operatorname{sinc}(\omega_{\text{BP}} \ell_{\text{BP}}/2) \cos(\omega_{\text{gw}} t_0 + \omega_{\text{BP}} (L + \ell_{\text{BP}}/2)) \Big] \quad (\text{C5c})$$

The length of the arms AP and BP is $\ell_{\text{AP}} = \ell_{\text{BP}} = L/(2 \sin(\pi/6 + \vartheta))$ used in the above equations. In the long wavelength approximations, $\omega_{\text{gw}} L/c \ll 1$ the sinc function can be taken as 1 and $\omega_{\text{arm}} \approx \omega_{\text{gw}}$. The differential time delay between the two photons in the two different arms, is $\Delta t_{\text{net}} = \Delta t_{\text{OA}} + \Delta t_{\text{AP}} - \Delta t_{\text{OB}} - \Delta t_{\text{BP}}$, and simplifying gives, Δt_{OA} and Δt_{AP} as,

$$c\Delta t_{\text{OA}} - c\Delta t_{\text{OB}} \approx L \left[\frac{\sqrt{3}}{4} (h_{xx} - h_{yy}) \cos(\omega_{\text{gw}}(t_0 + L/2)) \right],$$

$$c\Delta t_{\text{AP}} - c\Delta t_{\text{BP}} \approx \ell_{\text{AP}} \left[\frac{1}{2} \left((h_{xx} - h_{yy}) \cos\left(\frac{\pi}{6} - 2\vartheta\right) \right) \cos(\omega_{\text{gw}}(t_0 + L + \ell_{\text{AP}}/2)) \right],$$

and then the net time delay is given by,

$$c\Delta t_{\text{net}} \approx (h_{xx} - h_{yy}) \left[\frac{\sqrt{3}L}{4} \cos(\omega_{\text{gw}}(t_0 + L/2)) + \frac{\ell_{\text{AP}}}{2} \left(\cos\left(\frac{\pi}{6} - 2\vartheta\right) \right) \cos(\omega_{\text{gw}}(t_0 + L + \ell_{\text{AP}}/2)) \right]. \quad (\text{C7})$$

2. 3D pyramidal setup

We extend the analysis to the 3D pyramidal configuration proposed in the main text. We focus on "Detector 1," formed by the arms OAP and OBP. The time required for the photon to travel OAP, Δ_{OAP} to $\mathcal{O}(h^2)$ can be found by further splitting it into intervals Δt_{OA} and Δt_{AP} . Keeping O as the origin, the photon propagation directional vectors for each interval OA and AP are:

$$\hat{k}_{\text{OA}}^i = \left(\cos \frac{\pi}{12}, \sin \frac{\pi}{12}, 0 \right),$$

$$\hat{k}_{\text{AP}}^i = \left(\sin \frac{\pi}{12} \sin \vartheta - \cos \frac{\pi}{12}, \cos \frac{\pi}{12} \sin \vartheta - \sin \frac{\pi}{12}, \cos \vartheta \right).$$

Then the corresponding time delay for $\vartheta = \pi/6$ is given by,

$$c\Delta t_{\text{OA}} = L + \frac{L}{2} \left(h_{xx} \cos^2 \frac{\pi}{12} + h_{yy} \sin^2 \frac{\pi}{12} + 2h_{xy} \cos \frac{\pi}{12} \sin \frac{\pi}{12} \right) \operatorname{sinc}(\omega_{\text{OA}} L/2) \cos \omega_{\text{gw}} t_0 + \omega_{\text{OA}} L/2 \quad (\text{C8})$$

$$\begin{aligned}
c\Delta t_{AP} = L' + \frac{L'}{2} & \left(h_{xx} \left(\sin \frac{\pi}{12} \sin \vartheta - \cos \frac{\pi}{12} \right)^2 + h_{yy} \left(\cos \frac{\pi}{12} \sin \vartheta - \sin \frac{\pi}{12} \right)^2 + h_{zz} \cos^2 \vartheta \right. \\
& + 2h_{xy} \left(\sin \frac{\pi}{12} \sin \vartheta - \cos \frac{\pi}{12} \right) \left(\cos \frac{\pi}{12} \sin \vartheta - \sin \frac{\pi}{12} \right) + 2h_{xz} \left(\sin \frac{\pi}{12} \sin \vartheta - \cos \frac{\pi}{12} \right) \cos \vartheta \\
& \left. + 2h_{yz} \left(\cos \frac{\pi}{12} \sin \vartheta - \sin \frac{\pi}{12} \right) \cos \vartheta \right) \text{sinc}(\omega_{AP}L'/2) \cos \omega_{\text{gw}} t_0 + \omega_{AP}L'/2 \quad (\text{C9})
\end{aligned}$$

where, $\omega_{OA} = \omega_{\text{gw}}(1 - \cos[\pi/12 - \phi] \sin \theta)$ and $\omega_{AP} = \omega_{\text{gw}}(1 + \cos[\pi/12 - \phi] \sin \theta - \cos \theta \cos \vartheta - \sin \vartheta \sin \theta \sin[\pi/12 + \phi])$. Similarly, the time of flight of photon for the arm OBP can be found.

To maximize the response of the detector, we can use the long wavelength approximation $\omega_{\text{gw}}L/c \ll 1$ and the time delays can be simplified. Assuming that $L = L'$, and taking $\vartheta = \pi/6$ for symmetric configuration, the net time difference, $\Delta t_{\text{net}} = \Delta t_{OAP} - \Delta t_{OBP} = (\Delta t_{OA} - \Delta t_{OB}) + (\Delta t_{AP} - \Delta t_{BP})$ can be reduced to a simpler form.

$$\Delta t_{OA} - \Delta t_{OB} = \frac{\sqrt{3}L}{2c} (h_{xx} - h_{yy}) \quad (\text{C10})$$

$$\Delta t_{AP} - \Delta t_{BP} = \frac{L}{c} \left[\frac{1}{4} (h_{xx} + h_{yy}) + \frac{\sqrt{3}}{4} (h_{xx} - h_{yy}) + \sqrt{\frac{3}{2}} (h_{yz} - h_{xz}) - \frac{1}{2} h_{xy} \right] \quad (\text{C11})$$

Hence the net time delay due to the passage of gravitational wave in the HOM interferometer is given by,

$$\frac{c\Delta t_{\text{net}}}{L} = \frac{1}{4} (h_{xx} + h_{yy}) + \frac{3\sqrt{3}}{4} (h_{xx} - h_{yy}) + \sqrt{\frac{3}{2}} (h_{yz} - h_{xz}) + \frac{1}{2} h_{xy} \quad (\text{C12})$$

Here, the components of the metric h_{ij} are in the detector frame.

3. Antenna pattern function for 3D (Pyramidal) configuration

The gravitational wave strain signal $h(t)$ is defined as the fractional time delay, $h(t) \equiv c\Delta t_{\text{net}}/L_{\text{tot}}$. This scalar signal can be decomposed into the two polarization modes of the gravitational wave, h_+ and h_\times :

$$h(t) = F_+(\theta, \phi, \psi)h_+(t) + F_\times(\theta, \phi, \psi)h_\times(t), \quad (\text{C13})$$

where $F_{+,\times}$ are the antenna pattern functions, (θ, ϕ) define the propagation direction of the wave, and ψ is the polarization angle.

To derive $F_{+,\times}$, we transform the metric perturbation from the wave frame (where it is transverse-traceless) to the detector frame. The metric in the wave frame is:

$$h'_{\mu\nu} = \begin{pmatrix} h_+ & h_\times & 0 \\ h_\times & -h_+ & 0 \\ 0 & 0 & 0 \end{pmatrix}_{\text{wave}} . \quad (\text{C14})$$

The transformation to the detector frame is given by $h_{ij} = \mathcal{R}_{ik}\mathcal{R}_{jl}h'_{kl}$, where \mathcal{R} is the rotation matrix aligning the wave frame with the detector frame:

$$\mathcal{R}(\theta, \phi, \psi) = \begin{pmatrix} \cos \psi & \sin \psi & 0 \\ -\sin \psi & \cos \psi & 0 \\ 0 & 0 & 1 \end{pmatrix} \begin{pmatrix} \cos \theta & 0 & -\sin \theta \\ 0 & 1 & 0 \\ \sin \theta & 0 & \cos \theta \end{pmatrix} \begin{pmatrix} \cos \phi & \sin \phi & 0 \\ -\sin \phi & \cos \phi & 0 \\ 0 & 0 & 1 \end{pmatrix} . \quad (\text{C15})$$

Substituting the transformed components h_{ij} into Eq. (C9) and extracting the coefficients of h_+ and h_\times , we obtain the antenna pattern functions for Detector 1. Normalizing such that the maximum response is unity, we find:

$$\begin{aligned} F_+ \Big|_{D_1} = \frac{\sqrt{3}}{44} & \left[2\sqrt{6} \cos(2\psi) \sin(2\theta) (\cos \phi + \sin \phi) \right. \\ & + \cos(2\theta) \cos(2\psi) (\cos \phi + \sin \phi) ((1 + 3\sqrt{3}) \cos \phi + (1 - 3\sqrt{3}) \sin \phi) \\ & + \cos(2\psi) (-1 + 9\sqrt{3} \cos(2\phi) + 3 \sin(2\phi)) \\ & + 4\sqrt{6} \sin \theta (\cos \phi - \sin \phi) \sin(2\psi) \\ & \left. + 4 \cos \theta \sin(2\psi) (\cos(2\phi) - 3\sqrt{3} \sin(2\phi)) \right] , \end{aligned} \quad (\text{C16})$$

$$\begin{aligned} F_\times \Big|_{D_1} = \frac{\sqrt{3}}{44} & \left[-4\sqrt{6} \cos(2\psi) \sin \theta (\cos \phi - \sin \phi) \right. \\ & + \cos(2\theta) \sin(2\psi) (\cos \phi + \sin \phi) ((1 + 3\sqrt{3}) \cos \phi + (1 - 3\sqrt{3}) \sin \phi) \\ & + \sin(2\psi) (-1 + 9\sqrt{3} \cos(2\phi) + 3 \sin(2\phi)) \\ & + 2\sqrt{6} \sin(2\theta) (\cos \phi + \sin \phi) \sin(2\psi) \\ & \left. - 4 \cos \theta \cos(2\psi) (\cos(2\phi) - 3\sqrt{3} \sin(2\phi)) \right] . \end{aligned} \quad (\text{C17})$$

The corresponding antenna patterns for Detectors 2 and 3 are obtained by $\pm 120^\circ$ rotations

in the azimuth ϕ . The averaged response of the full network is discussed in the main text.

- [1] P. W. Milonni, *The Quantum vacuum: An Introduction to quantum electrodynamics* (Academic Press, 1994).
- [2] C. Cohen-Tannoudji, J. Dupont-Roc, and G. Grunberg, *Photons and Atoms: Introduction to quantum electrodynamics* (1987).
- [3] M. E. Peskin and D. V. Schroeder, *An Introduction to quantum field theory* (Addison-Wesley, Reading, USA, 1995).
- [4] L. Mandel and E. Wolf, *Optical Coherence and Quantum Optics* (Cambridge Univ. Pr., 1995).
- [5] P. R. Saulson, *Fundamentals of Interferometric Gravitational Wave Detectors*, 2nd ed. (World Scientific, 2017).
- [6] B. P. Abbott *et al.* (LIGO Scientific, Virgo), *Phys. Rev. Lett.* **116**, 061102 (2016), arXiv:1602.03837 [gr-qc].
- [7] L. S. Finn, *Phys. Rev. D* **79**, 022002 (2009), arXiv:0810.4529 [gr-qc].
- [8] N. Aggarwal *et al.*, *Living Rev. Rel.* **24**, 4 (2021), arXiv:2011.12414 [gr-qc].
- [9] T. Rothman and S. Boughn, *Found. Phys.* **36**, 1801 (2006), arXiv:gr-qc/0601043.
- [10] S. Boughn and T. Rothman, *Class. Quant. Grav.* **23**, 5839 (2006), arXiv:gr-qc/0605052.
- [11] C. J. Hogan, *Phys. Rev. D* **77**, 104031 (2008), arXiv:0712.3419 [gr-qc].
- [12] F. Dyson, *Int. J. Mod. Phys. A* **28**, 1330041 (2013).
- [13] T. Bringmann, V. Domcke, E. Fuchs, and J. Kopp, *Phys. Rev. D* **108**, L061303 (2023), arXiv:2304.10579 [hep-ph].
- [14] J. Gräfe, F. Adamietz, and R. Schützhold, *Phys. Rev. D* **108**, 064056 (2023), arXiv:2302.14694 [quant-ph].
- [15] R. Schützhold, *Phys. Rev. Lett.* **135**, 171501 (2025), arXiv:2502.10221 [gr-qc].
- [16] C. K. Hong, Z. Y. Ou, and L. Mandel, *Phys. Rev. Lett.* **59**, 2044 (1987).
- [17] S. N. Gupta, *Phys. Rev.* **96**, 1683 (1954).
- [18] R. P. Feynman, *Feynman lectures on gravitation*, edited by F. B. Morinigo, W. G. Wagner, and B. Hatfield (1996).
- [19] J. Aasi *et al.* (LIGO Scientific), *Class. Quant. Grav.* **32**, 074001 (2015), arXiv:1411.4547 [gr-qc].
- [20] F. Acernese *et al.* (VIRGO), *Class. Quant. Grav.* **32**, 024001 (2015), arXiv:1408.3978 [gr-qc].

- [21] Y. Aso, Y. Michimura, K. Somiya, M. Ando, O. Miyakawa, T. Sekiguchi, D. Tatsumi, and H. Yamamoto (KAGRA), *Phys. Rev. D* **88**, 043007 (2013), arXiv:1306.6747 [gr-qc].
- [22] R. Schnabel, N. Mavalvala, D. E. McClelland, and P. K. Lam, *Nature Commun.* **1**, 121 (2010), arXiv:2411.07313 [quant-ph].
- [23] S. Dimopoulos, P. W. Graham, J. M. Hogan, M. A. Kasevich, and S. Rajendran, *Phys. Rev. D* **78**, 122002 (2008), arXiv:0806.2125 [gr-qc].
- [24] L. Badurina *et al.*, *JCAP* **05**, 011 (2020), arXiv:1911.11755 [astro-ph.CO].
- [25] J.-W. Pan, Z.-B. Chen, C.-Y. Lu, H. Weinfurter, A. Zeilinger, and M. Żukowski, *Rev. Mod. Phys.* **84**, 777 (2012), arXiv:0805.2853 [quant-ph].
- [26] Y. Chen, A. Pai, K. Somiya, S. Kawamura, S. Sato, K. Kokeyama, and R. L. Ward, *Phys. Rev. Lett.* **97**, 151103 (2006), arXiv:gr-qc/0603054.
- [27] S. Sato, S. Kawamura, K. Kokeyama, R. L. Ward, Y. Chen, A. Pai, and K. Somiya, *Phys. Rev. Lett.* **98**, 141101 (2007), arXiv:gr-qc/0608095.
- [28] M. Liu and B. Gong, *Sci. Rep.* **10**, 16285 (2020), arXiv:2001.06129 [gr-qc].
- [29] H.-B. Jin and C.-F. Qiao, *Sci. China Phys. Mech. Astron.* **68**, 220414 (2025), arXiv:2405.03492 [gr-qc].
- [30] C. M. Caves, *Phys. Rev. D* **23**, 1693 (1981).